PHYSICAL REVIEW B **80**, 035125 (2009)

Exchange-correlation energy functional based on the Airy-gas reference system

Lucian A. Constantin, Adrienn Ruzsinszky, and John P. Perdew
Department of Physics and Quantum Theory Group, Tulane University, New Orleans, Louisiana 70118, USA

(Received 11 January 2009; revised manuscript received 12 May 2009; published 23 July 2009)

In recent work, generalized gradient approximations (GGAs) have been constructed from the energy density of the Airy gas for exchange but not for correlation. We report the random-phase approximation (RPA) conventional correlation energy density of the Airy gas, the simplest edge electron gas, in which the auxiliary noninteracting electrons experience a linear potential. By fitting the Airy-gas RPA exchange-correlation energy density and making an accurate short-range correction to RPA, we propose a simple beyond RPA GGA density functional ("ARPA+") for the exchange-correlation energy. Our functional, tested for jellium surfaces, atoms, molecules, and solids, improves mildly over the local spin-density approximation for atomization energies and lattice constants without much worsening the already good surface exchange-correlation energies.

DOI: 10.1103/PhysRevB.80.035125 PACS number(s): 71.10.Ca, 71.15.Mb, 71.45.Gm

I. INTRODUCTION

In Kohn-Sham[1] (KS) density-functional theory, the ground-state density, and energy of interacting electrons in a scalar external potential $v(\mathbf{r})$ are computed efficiently via a self-consistent calculation for an auxiliary system of noninteracting electrons in a scalar effective potential $v_{eff}(\mathbf{r})$. Once the exchange-correlation (xc) energy as a functional of the electron density has been approximated, its functional derivative provides the exchange-correlation contribution to $v_{eff}(\mathbf{r})$. By itself, the deviation of $v_{eff}(\mathbf{r})$ from the constant chemical potential determines the electron density and thus the exchange-correlation energy. Typical approximations are designed to be exact for a reference system, most often the uniform electron gas in which the auxiliary noninteracting electrons see a constant or uniform v_{eff}. Sometimes additional exact constraints or fits to experiment are also built into the approximation. Recently Kohn and Mattsson[2] have proposed as a more realistic reference system, the edge electron gas, in which $v_{eff}(\mathbf{r})$ varies more or less linearly near the edge surface of the density. While the uniform gas could be (and is) a good reference for a bulk solid, the edge electron gas could be at least as good for a bulk solid and better for solid surfaces, molecules, and atoms, which have regions where the electron-density evanesces.

The edge surface of any electron system is defined[2] by $v_{eff}(\mathbf{r})=\mu$, where $v_{eff}(\mathbf{r})$ is the exact KS (Ref. 1) effective potential and μ is the chemical potential. Outside this classical turning surface, all noninteracting electrons tunnel into a barrier. The simplest example of an edge electron gas is the Airy gas, where any electron feels a linear effective potential[2] and thus the normalized one-particle eigenfunctions are proportional to the Airy function. The Airy gas has not only a surface-like region but also a region of high and slowly varying (Thomas-Fermi-type) electron density where the local-density approximation (with uniform-gas input) is accurate[2,3] for the noninteracting kinetic, exchange, and correlation energy densities.

The Airy gas has appeared before in density-functional theory: (1) the effective finite-linear-potential model gives remarkably good results for the jellium surface problem, where the orbitals of this model are approximated with plane waves inside the bulk, Airy functions near the surface, and exponential functions far in the vacuum.[4–6] (2) Baltin[7] constructed a generalized gradient approximation (GGA) for the orbital kinetic energy from the Airy-gas kinetic energy density but his approximation does not recover the second-order gradient expansion for the kinetic energy density[8,9] and is poor for atoms and molecules.[10,11] However, the kinetic energy density of the Airy gas[11] can still be a starting point for construction of GGA kinetic energy functionals that can be more accurate for atoms, molecules, jellium clusters, and jellium surfaces.[11,12] The trick is to fit a GGA *plus a* $\nabla^2 n$ term integrating to zero to the Airy-gas kinetic energy density.

The exchange energy density of the Airy gas[2] was fitted[13,14] with a function dependent on the density and its gradient. Thus, Vitos *et al.*[13] developed a GGA exchange energy functional (LAG or local Airy-gas GGA) that was used with the local spin-density approximation (LSDA) correlation energy. This xc energy functional gives results for atoms very close to, but better than, the LSDA ones, and its accuracy for atomization energy of diatomic molecules is similar to that of the Perdew-Burke-Ernzerhof or PBE GGA (Ref. 15) while for bulk systems the results of LAG GGA are close to the PBEsol GGA[16] and to experimental values. However, the jellium xc surface energies of LAG are far too low (lower even than those of the PBE GGA). Armiento and Mattsson[14,17] proposed an xc energy functional (AM05 GGA) using a better fit for the Airy-gas exchange energy density and a correlation energy functional constructed such that the AM05 xc jellium surface energies fit the RPA+ (Ref. 18) values (random phase approximation or RPA plus a GGA short-range correction). AM05 is also based on the subsystem functional approach,[19] which permits an interpolation between a uniform-gas reference for the bulk of a solid and an Airy-gas reference for the surface. (Since the Airy-gas reference system by itself provides such an interpolation, we make no further interpolation here.) AM05 slightly improves the accuracy of LAG GGA for bulk systems.

Because the correlation energy density of the Airy gas was unknown, the LAG GGA and AM05 GGA used in their construction only the Airy-gas exchange energy density. In this paper we compute the correlation energy density of the Airy gas in the RPA and fit it to a GGA (Airy-gas RPA or ARPA GGA). As in Refs. 13 and 14, our fit is made without regard to exact constraints on $E_{\mathrm{xc}}[n_\uparrow, n_\downarrow]$. The Airy gas is a system of delocalized electrons where the self-interaction correction has no effect and where the GGA correction[18] to the integrated RPA energy should be accurate. Our functional, including this GGA correction to RPA, will be called ARPA+.

Unlike energies, energy densities of nonuniform systems are not unique. It is not clear to us that the conventional choice for the exchange-correlation energy density (made in Refs. 13 and 14 and here) is optimal. It is not our intention here to either endorse or criticize this choice but simply to see what GGA is obtained from the Airy-gas reference system within a consistent implementation for correlation as well as exchange.

AM05, PBEsol, and ARPA+ are of special interest as candidates for a "GGA for solids" providing better lattice constants and surface energies than standard GGA's such as PBE, possibly at the cost of a worsened description of atoms and molecules. There have been several recent papers commenting on or testing for solids the LAG, AM05, and PBEsol GGAs.[20–24]

Our paper is organized as follows. In Sec. II, we propose a simple model for the Airy gas. In Sec. III, we construct the ARPA+GGA xc energy functional from our Airy-gas model. In Sec. IV we test the ARPA+GGA for atoms, molecules, jellium surfaces, and bulk solids. In Sec. V, we summarize our conclusions.

II. AIRY-GAS MODEL

The simplest example of an edge electron gas is the Airy gas that is translationally invariant in the plane of the surface ($z=0$) and has the effective potential[2,25]

$$v_{eff}(z) = \begin{cases} -Fz, & -\infty < z < L \quad (F>0) \\ \infty, & z \geq L \quad (L/l \to \infty) \end{cases} . \tag{1}$$

Here $F=|dv_{eff}(z)/dz|$ is the slope of the effective potential and the characteristic length scale

$$l=(2F)^{-1/3} \tag{2}$$

is approximately the edge region thickness.[2] (Unless otherwise stated, atomic units are used throughout, i.e., $e^2=\hbar=m_e=1$.)

The KS orbitals are $\Psi_{j,\mathbf{k}_\parallel}(\mathbf{r})=\phi_j(z)\frac{1}{\sqrt{A}}e^{i\mathbf{k}_\parallel\mathbf{r}_\parallel}$, where $\mathbf{k}_\parallel$ and $\mathbf{r}_\parallel$ are the wave vector and the position vector parallel to the plane of the surface, A is the cross-sectional area, and the orthonormal eigenfunctions $\phi_j(z)$ satisfy the equation

$$\left(-\frac{1}{2}\frac{d^2}{dz^2}-Fz-\epsilon_j\right)\phi_j(z)=0 \tag{3}$$

with the boundary conditions

$$\phi_j(-\infty)=\phi_j(L)=0. \tag{4}$$

They are given by the Airy functions

$$\phi_j(z)=a\mathrm{Ai}\left(-\frac{z}{l}-\frac{\epsilon_j}{\epsilon}\right), \tag{5}$$

where $\epsilon=(F^2/2)^{1/3}$ is the Airy gas characteristic energy scale, a is the normalization constant, and ϵ_j is the jth eigenvalue calculated from the boundary condition $\phi_j(L)=0$. The Airy-gas density is

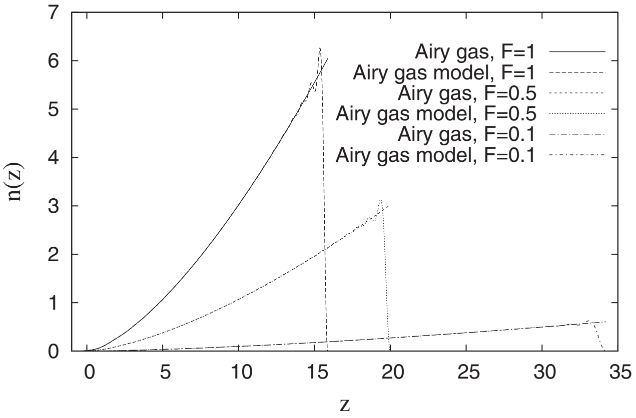

FIG. 1. Electron density (electrons/bohr^3) of the Airy gas and of our model versus z (bohr) for several slopes of the effective potential ($F=0.1$ making $l=1.710$, $F=0.5$ making $l=1.000$, and $F=1$ making $l=0.793$). The edge is at $z=0$.

$$n(z)=\sum_j^{occ}\phi_j^2(z)|\epsilon_j|/\pi. \tag{6}$$

We recall that all three-dimensional states with energy up to $\mu=0$ are occupied. Thus the Airy gas is completely determined by the length l and the energy ϵ.

In the limit $L/l\to\infty$, the normalization constant is[2]

$$a=\frac{\pi^{1/2}}{(Ll)^{1/4}}, \tag{7}$$

and the eigenvalues are[2]

$$\epsilon_j=-j\left(\frac{l}{L}\right)^{1/2}\pi\epsilon. \tag{8}$$

So, the density of the Airy gas is

$$n(z)=l^{-3}n_0(\eta), \quad \eta=z/l, \tag{9}$$

where

$$n_0(\eta)=\frac{1}{2\pi}\int_0^\infty \mathrm{Ai}^2(\eta'-\eta)\eta' d\eta'. \tag{10}$$

Let us consider a model for the Airy gas that is described by Eqs. (1)–(6) but instead of choosing $L/l\to\infty$ we take $L/l=20$ for computational convenience. Such a system has 19 occupied orbitals $\phi_j(z)$ and can accurately describe the Airy gas. The normalization constants of Eq. (5) and the eigenvalues ϵ_j are computed numerically. Such an approach is similar to jellium slabs that are described by a finite number of occupied orbitals in the z direction and that can accurately predict the surface energies of semi-infinite jellium surfaces.[26]

We select three values $F=0.1$, $F=0.5$, and $F=1$ for the slope of the effective potential. The accuracy of the model does not depend on the F value. In Fig. 1 we show the densities of the Airy gas and of our Airy-gas model for the chosen values of the slope F. We see the exact Airy-gas

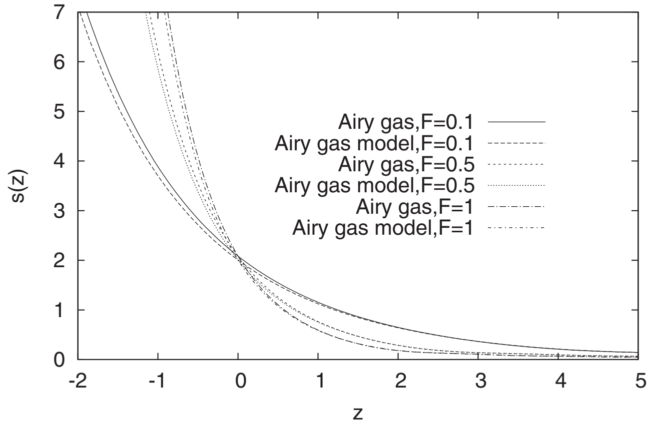

FIG. 2. Reduced gradient $s(z)$ versus z, of the Airy gas and our model, for several slopes of the effective potential ($F=0.1$, 0.5, and 1.) The edge is at $z=0$.

densities and the modeled ones cannot be distinguished until $z \sim L = 20 \cdot l$ where the densities of our model have oscillations until they vanish.

Important ingredients of any GGA functional are the density $n(\mathbf{r})$ and the reduced density gradient

$$s(\mathbf{r}) = |\nabla n(\mathbf{r})| / [2k_F(\mathbf{r})n(\mathbf{r})], \qquad (11)$$

where $k_F(\mathbf{r}) = [3\pi^2 n(\mathbf{r})]^{1/3}$ is the Fermi wave vector. (The dimensionless density gradient $s(\mathbf{r})$ measures the variation in the density over a Fermi wavelength $\lambda_F = 2\pi/k_F$.) In Fig. 2 we compare the reduced gradients of our model and of the exact Airy gas. Up to $s=2$, the model nicely matches the exact Airy gas and it is accurate for any value of s. (We note that s values bigger than 3 are found in the tail of an atom or molecule, where the electron density is negligible. We also note that in most bulk solids the maximum[24] value of the reduced gradient is smaller than 2.) Figures 1 and 2 demonstrate that our model is accurate and thus we can use it for the calculation of the Airy-gas correlation energy.

III. RPA CORRELATION ENERGY DENSITY OF THE AIRY GAS AND THE CONSTRUCTION OF THE ARPA+GGA

The conventional xc energy density at a point is $n\epsilon_{xc}$, where n is the local electron density and ϵ_{xc} is the conventional xc energy per particle. Let us consider the spin-unpolarized Airy-gas model with the edge plane at $z=0$. Using its translational invariance in a plane perpendicular to the z axis and the so-called adiabatic-connection fluctuation-dissipation theorem,[26–29] the exact expression for the conventional xc energy per particle at point z is[26–28]

$$\epsilon_{xc}(z) = \frac{1}{2}\int \frac{d\mathbf{q}_{\parallel}}{(2\pi)^2}\int d\acute{z}\; v(z,\acute{z},q_{\parallel})\left[-\frac{1}{\pi n(z)} \times \int_0^1 d\lambda \int_0^{\infty} d\omega\, \chi^{\lambda}(z,\acute{z};q_{\parallel},i\omega) - \delta(z-\acute{z})\right], \qquad (12)$$

where $\mathbf{q}_{\parallel}$ is the wave vector parallel to the surface, and χ^{λ} and v are the two-dimensional Fourier transforms of the interacting density response function at the coupling strength λ and of the Coulomb potential, respectively. The substitution of χ^{λ} with the noninteracting density response function χ^0 into Eq. (12) yields the exact $\epsilon_x(z)$ (expressible in terms of occupied orbitals only, although χ^0 also requires the unoccupied orbitals). The density response function obeys the screening integral Dyson-type equation[30]

$$\chi^{\lambda}(\mathbf{r},\mathbf{r}',\omega) = \chi^0(\mathbf{r},\mathbf{r}',\omega) + \int d\mathbf{r}_1 d\mathbf{r}_2 \chi^0(\mathbf{r},\mathbf{r}_1,\omega) \times \{v^{\lambda}(\mathbf{r}_1,\mathbf{r}_2) + f_{xc}^{\lambda}[n](\mathbf{r}_1,\mathbf{r}_2,\omega)\}\chi^{\lambda}(\mathbf{r}_2,\mathbf{r}',\omega), \qquad (13)$$

where $v^{\lambda}(\mathbf{r}_1,\mathbf{r}_2) = \lambda/|\mathbf{r}_1 - \mathbf{r}_2|$ and $f_{xc}^{\lambda}[n](\mathbf{r}_1,\mathbf{r}_2,\omega) = \delta v_{xc}^{\lambda}[n](\mathbf{r}_1,\omega)/\delta n(\mathbf{r}_2,\omega)$ is the exact xc kernel. Here $v_{xc}^{\lambda}[n]$ is the exact frequency-dependent xc potential at coupling strength λ. Obviously, the exact xc kernel is unknown and it has to be approximated. Approximations of the xc kernel are usually constructed from the uniform electron gas[31–33] and have not been tested sufficiently for nonuniform systems. When $f_{xc}^{\lambda}[n](\mathbf{r},\mathbf{r}';\omega)$ is taken to be zero, Eq. (13) reduces to the RPA. The RPA xc hole density is exact at large interelectronic separations such that it can correctly describe the xc hole density of an electron far outside of a jellium surface[34] and its on-top hole is finite and well described by the LSDA-RPA (Ref. 18) on-top hole in the case of a jellium surface.[34]

Equations (12) and (13) can be generalized[35] for systems with any relative spin polarization

$$\zeta = \frac{n_{\uparrow} - n_{\downarrow}}{n_{\uparrow} + n_{\downarrow}}, \qquad (14)$$

where $n_{\uparrow}$ and $n_{\downarrow}$ are the spin densities, $n_{\uparrow} + n_{\downarrow} = n$. Thus for the Airy-gas model, we choose to calculate the RPA correlation energy per particle at point z, from Eqs. (12) and (13), and to add the RPA+ short-range correction,

$$E_{xc}^{\text{RPA+}} = E_{xc}^{\text{RPA}} + (E_{xc}^{\text{GGA}} - E_{xc}^{\text{GGA-RPA}}), \qquad (15)$$

where E_{xc}^{GGA} is the PBE GGA (Ref. 15) xc energy and $E_{xc}^{\text{GGA-RPA}}$ is the PBE-RPA GGA xc energy.[18] The exchange contribution and the long-range correlation contribution cancel out of the bracketed term in Eq. (15), leaving only short-range correlation. Because the self-interaction correction is not important for the Airy gas, Eq. (15) will give nearly the exact correlation energy of the Airy gas.

For the numerical evaluation of Eqs. (12) and (13), we follow the method described in Refs. 26 and 36 but instead of using the double-cosine and single-cosine representations of the density response function and the density, respectively, we use a grid on the z axis for $\chi^{\lambda}(z,\acute{z};q_{\parallel},i\omega)$ and $n(z)$. We find that the first 50 unoccupied orbitals $\phi_j(z)$ are enough for an accurate calculation. (Our grid on the z axis can accurately describe the occupied and the first 50 unoccupied orbitals[37]).

The exchange energy for a spin-polarized system may be evaluated from the spin-unpolarized version using the spin-scaling relation,[38]

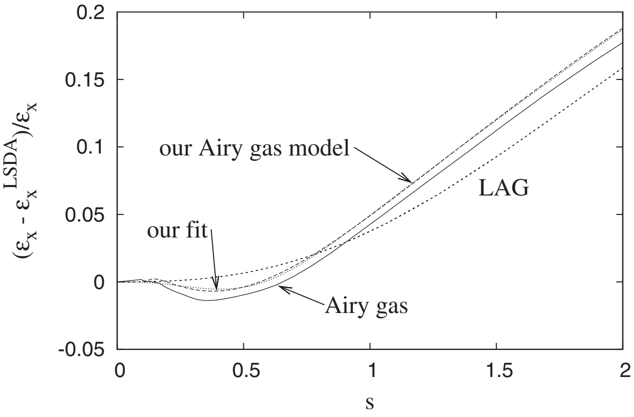

FIG. 3. $(\epsilon_x - \epsilon_x^{\rm LSDA})/\epsilon_x$ versus the reduced gradient s for the Airy-gas model, the Airy gas, the LAG GGA (Ref. 13) and for our fit [see Eqs. (17) and (18)]. The "Airy-gas" curve uses ϵ_x and $\epsilon_x^{\rm LSDA}$ of the Airy gas, whereas the other non-LAG curves use ϵ_x and $\epsilon_x^{\rm LSDA}$ of our model for the Airy gas. The AM05 GGA (Ref. 14), not shown in the figure, has the same behavior as the LAG GGA.

$$E_x[n_\uparrow,n_\downarrow] = \frac{1}{2}\{E_x[2n_\uparrow] + E_x[2n_\downarrow]\}, \tag{16}$$

and thus we only need to consider the spin-unpolarized case. We fit the exchange energy per particle of the Airy-gas model, using the nonlinear least-square Levenberg-Marquardt method[39] with the following expression:

$$\epsilon_x^A(n(\mathbf{r})) = \epsilon_x^{\rm LSDA}(n(\mathbf{r}))F_x^A(s(\mathbf{r})), \tag{17}$$

where $\epsilon_x^{\rm LSDA} = -3k_F/4\pi$ and the enhancement factor is

$$F_x^A = \frac{a_1 s^{a_2}}{(1+a_3 s^{a_2})^{a_4}} + \frac{1 - a_5 s^{a_6} + a_7 s^{a_8}}{1 + a_9 s^{a_{10}}}, \tag{18}$$

where $a_1 = 0.041106$, $a_2 = 2.626712$, $a_3 = 0.092070$, and $a_4 = 0.657946$ are the parameters found in Ref. 13 and $a_5 = 133.983631$, $a_6 = 3.217063$, $a_7 = 136.707378$, $a_8 = 3.223476$, $a_9 = 2.675484$, and $a_{10} = 3.473804$ are parameters found from our fitting procedure. Equation (17) recovers the correct LSDA for the uniform electron gas and fits well the Airy-gas exchange energy per particle for $s \le 20$. (Values of s bigger than 20 are found only when the density is negligible. We recall that the local Airy approximation or LAA GGA of Ref. 14 is a better fit than LAG or ϵ_x^A far outside the edge.)

In Fig. 3 we show $(\epsilon_x - \epsilon_x^{\rm LSDA})/\epsilon_x$ versus the reduced gradient s for several approximations. The Airy-gas curve as well as our Airy-gas model curve have a negative region around $s \approx 0.5$ that was not taken into account by the LAG GGA and AM05 GGA. We find this fine feature only because we plot $(\epsilon_x - \epsilon_x^{\rm LSDA})/\epsilon_x$ instead of ϵ_x. (This feature can also be seen in the inset of Fig. 1 of Ref. 14 but it was not taken into account in the construction of AM05.) The second term on the right-hand side of Eq. (18) models the exact behavior at small reduced gradients, whereas the first term on the right-hand side of Eq. (18) has the same form as the parametrization proposed in Ref. 13. We observe that our fit [Eqs. (17) and (18)] is very close to the exact Airy-gas model as well as to the exact Airy-gas exchange energy per particle.

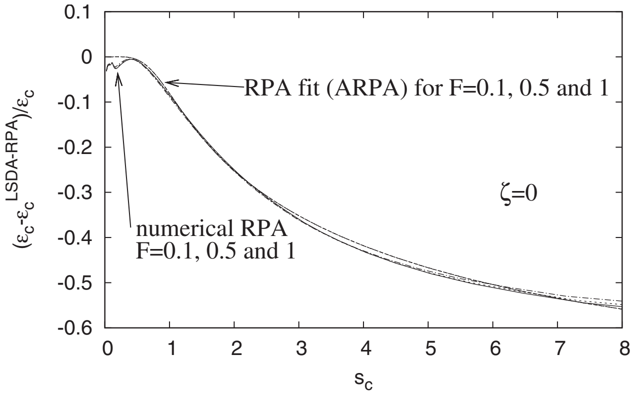

FIG. 4. $(\epsilon_c - \epsilon_c^{\rm LSDA\text{-}RPA})/\epsilon_c$ of the spin-unpolarized ($\zeta = 0$) Airy-gas model versus s_c [see Eq. (20)] for numerical RPA and our fit ARPA of Eq. (19) for several slopes of the effective potential ($F = 0.1$, 0.5, and 1). Note that the numerical RPA has errors of order 2% in the region of small reduced gradient s_c.

We fit the RPA correlation energy per particle of the Airy gas of any spin polarization with the following expression, using again the nonlinear least-square Levenberg-Marquardt method[39]

$$\epsilon_c^{\rm ARPA}(r_s,\zeta,s_c) = \epsilon_c^{\rm LSDA\text{-}RPA}(r_s,\zeta)F_c(s_c), \tag{19}$$

where r_s is the local Wigner-Seitz radius $[n = 3/(4\pi r_s^3) = k_F^3/3\pi^2]$, ζ is the relative spin polarization of Eq. (14), $\epsilon_c^{\rm LSDA\text{-}RPA}$ is the RPA correlation energy per particle of the uniform electron gas (see Ref. 40), and

$$s_c(\mathbf{r}) = \phi|\nabla n(\mathbf{r})|/[2(3\pi^2)^{1/3}n(\mathbf{r})^{7.9/6}] \tag{20}$$

with $\phi = [(1+\zeta)^{2/3} + (1-\zeta)^{2/3}]/2$ being a spin-scaling factor. The correlation enhancement factor is

$$F_c = \frac{1 + b_1 s_c^3 + b_2 s_c^4}{1 + b_3 s_c^3 + b_4 s_c^4} \tag{21}$$

with $b_1 = 1.01453936$, $b_2 = 0.3255243$, $b_3 = 0.941597104$, and $b_4 = 0.587664306$. Equation (21) is a simple Padé approximation that recovers the RPA behavior of the uniform electron gas when $s_c = 0$. All the parameters were found by the fitting procedure and not by constraints on the integrated correlation energy [which would suggest[15] an exponent of 7/6 and the appearance of ϕ in the denominator of Eq. (20) and a quadratic term in the small-gradient expansion of Eq. (21)]. The irrelevance of some standard constraints may be related to the absence[41] of a second-order gradient expansion for the conventional correlation energy density. Given F, $\epsilon_c^{\rm RPA}$ is a function of z, and s_c is a monotonic (hence invertible) function of z, so $\epsilon_c^{\rm RPA}$ can be expressed as a function of s_c. Since there is a one-to-one correspondence between the $\epsilon_c^{\rm RPA}$ and our $\epsilon_c^{\rm ARPA}$, we can do the fitting. The fitting was done for s_c between 0 and 20.

In Figs. 4 and 5 we show $(\epsilon_c - \epsilon_c^{\rm LSDA\text{-}RPA})/\epsilon_c$ versus s_c for the spin-unpolarized Airy-gas model ($\zeta = 0$) and fully spin-polarized Airy-gas model ($\zeta = 1$), respectively, for the slopes of the effective potential used in Figs. 1 and 2 ($F = 0.1$, 0.5, and 1). We note that our numerical calculation is accurate for $s_c \gtrsim \sim 0.3$, see Ref. 37. We see in both figures that the nu-

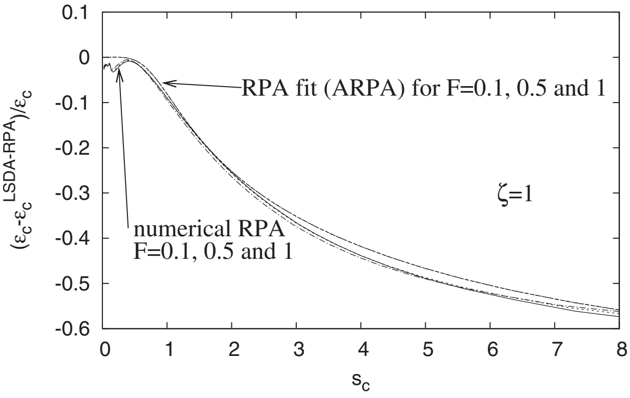

FIG. 5. $(\epsilon_c-\epsilon_c^{\text{LSDA-RPA}})/\epsilon_c$ of the fully spin-polarized ($\zeta=1$) Airy-gas model versus s_c for numerical RPA and our fit ARPA of Eq. (19) for several slopes of the effective potential ($F=0.1$, 0.5, and 1). Note that the numerical RPA has errors of order 2% in the region of small reduced gradient s_c.

merical RPA correlation energy density does not depend much on the slope value F when plotted against s_c, motivating our definition of s_c in Eq. (20) and making the fit of the RPA correlation energy per particle independent of the F value[42] [see Eqs. (19) and (21)]. For $s_c\leq 0.5$ the ARPA of Eq. (19) is close to exact even if it does not match well the detailed numerical behavior, as it does in the region $0.5\leq s_c\leq 10$.

Overall we consider

$$\epsilon_{\text{xc}}^{\text{ARPA}}=\epsilon_x^{A}+\epsilon_c^{\text{ARPA}} \tag{22}$$

an xc GGA functional that fits very well the Airy-gas RPA xc energy density. Thus making the RPA+ short-range correction [see Eq. (15)] to ARPA GGA, we propose the following GGA xc functional (ARPA+GGA) constructed from the Airy gas

$$\epsilon_{\text{xc}}^{\text{ARPA+}}=\epsilon_{\text{xc}}^{\text{ARPA}}+(\epsilon_c^{\text{PBE}}-\epsilon_c^{\text{PBE-RPA}}). \tag{23}$$

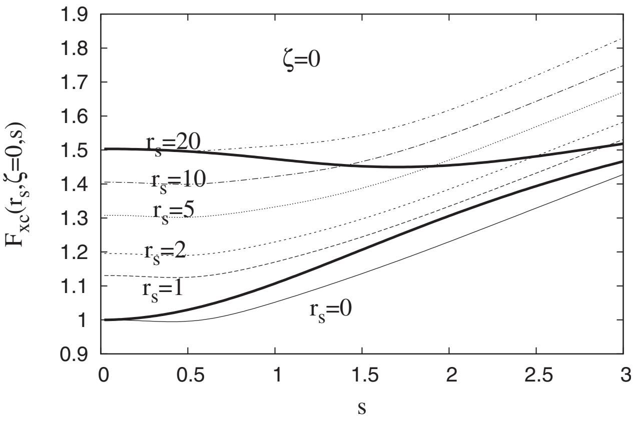

FIG. 6. Enhancement factor F_{xc} [see Eq. (24)] for the spin-unpolarized case ($\zeta=0$), as a function of the reduced gradient s for several values of r_s ($r_s=0$, 1, 2, 5, 10, and 20). The thin lines represent the ARPA+ enhancement factor whereas the thick lines are the PBEsol enhancement factor for $r_s=0$ and $r_s=20$, respectively. The LSDA is $F_{\text{xc}}(r_s,\zeta=0,s=0)$.

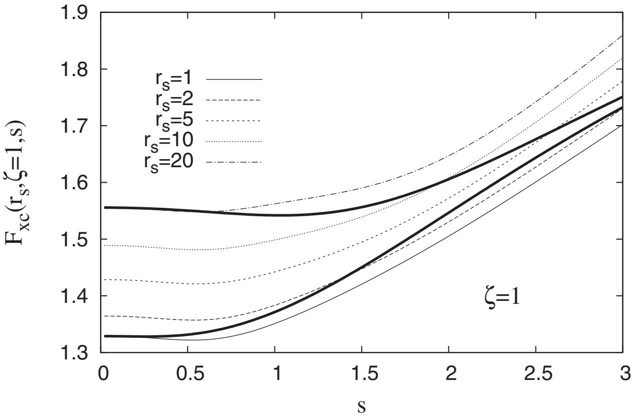

FIG. 7. Enhancement factor F_{xc} [see Eq. (24)] for the fully spin-polarized case ($\zeta=1$), as a function of the reduced gradient s for several values of r_s ($r_s=1$, 2, 5, 10, and 20). The thin lines represent the ARPA+ enhancement factor whereas the thick lines are the PBEsol enhancement factor for $r_s=1$ and $r_s=20$, respectively. The LSDA is $F_{\text{xc}}(r_s,\zeta=1,s=0)$.

The nonlocality of a GGA is displayed by the enhancement factor[43,44]

$$F_{\text{xc}}^{\text{GGA}}=\frac{\epsilon_{\text{xc}}^{\text{GGA}}(n_\uparrow,n_\downarrow,\nabla n_\uparrow,\nabla n_\downarrow)}{\epsilon_x^{unif}(n)}, \tag{24}$$

$\epsilon_x^{unif}(n)$ being the exchange energy per particle of a spin-unpolarized uniform electron gas. For a spin-unpolarized system in the high-density limit ($r_s\to 0$), the exchange energy is dominant and Eq. (24) defines the exchange enhancement factor $F_x^{\text{GGA}}=\epsilon_x^{\text{GGA}}(n_\uparrow,n_\downarrow,\nabla n_\uparrow,\nabla n_\downarrow)/\epsilon_x^{unif}(n)$. Figures 6 and 7 show the enhancement factor of ARPA+ compared to PBEsol as a function of the reduced gradient s, for several values of r_s, in the spin-unpolarized case and the fully spin-polarized case, respectively. In both figures, the ARPA+ and PBEsol enhancement factors agree well at small gradients (for $s\leq 0.5$) but for $s\gg 0.5$ ARPA+ shows more exchange-correlation nonlocality than PBEsol at low density, and less at high density.

Figures 8 and 9 show a comparison between the ARPA

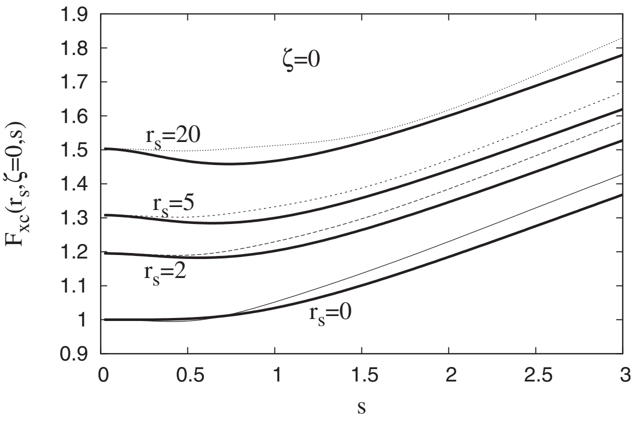

FIG. 8. Comparison of $F_{\text{xc}}^{\text{ARPA+}}(r_s,\zeta=0,s)$ (shown with thin lines) and $F_{\text{xc}}^{\text{AM05}}(r_s,\zeta=0,s)$ (shown with thick lines) for several values of r_s ($r_s=0$, 2, 5, and 20).

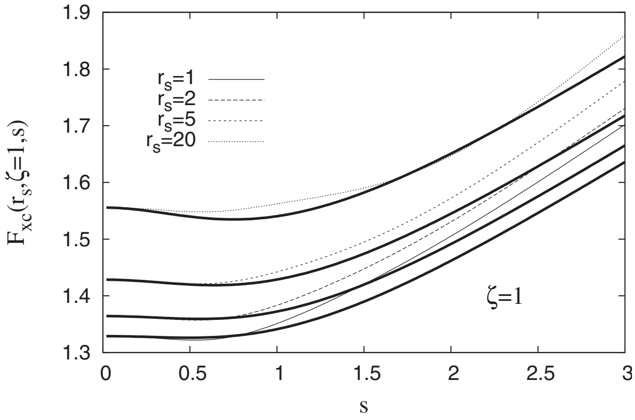

FIG. 9. Comparison of $F_{\mathrm{xc}}^{\mathrm{ARPA+}}(r_s,\zeta=1,s)$ (shown with thin lines) and $F_{\mathrm{xc}}^{\mathrm{AM05}}(r_s,\zeta=1,s)$ of Ref. 17 (shown with thick lines) for several values of r_s (r_s=1, 2, 5, and 20).

+GGA and AM05 GGA enhancement factors for the spin-unpolarized and fully spin-polarized cases. Up to $s=0.5$, $F_{\mathrm{xc}}^{\mathrm{ARPA+}}(r_s,\zeta,s)$ and $F_{\mathrm{xc}}^{\mathrm{AM05}}(r_s,\zeta,s)$ agree very well. For $s \geq 0.5$, $F_{\mathrm{xc}}^{\mathrm{ARPA+}}(r_s,\zeta,s)$ shows slightly more nonlocality than $F_{\mathrm{xc}}^{\mathrm{AM05}}(r_s,\zeta,s)$ and, even if this difference is small, it has noticeable effects for the lattice constants of bulk solids. Overall, our ARPA+ confirms the AM05 construction for correlation.

IV. TESTS OF THE ARPA+GGA xc ENERGY FUNCTIONAL

In this section we test our functionals for jellium surfaces, atoms, molecules, and bulk solids. The calculations use the spin-scaling relation of Eq. (16).

A. Jellium surfaces

TABLE I. Jellium surface exchange and exchange-correlation energies (erg/cm^2) for LSDA, PBE, and ARPA+ in and beyond the random-phase approximation. We also show the jellium surface exchange and exchange-correlation energies beyond RPA for LAG GGA, AM05 GGA, PBEsol GGA, and TPSS meta-GGA of Ref. 47. The exact values of σ_x^{exact} and $\sigma_{\mathrm{xc}}^{\mathrm{RPA}}$ are from Ref. 26 and the fixed-node diffusion Monte Carlo (DMC) $\sigma_{\mathrm{xc}}^{\mathrm{DMC}}$ values are interpolations and extrapolations of the estimates of Ref. 48 (see Table 2 of Ref. 49). To interpolate or extrapolate r_s we recommend Eq. (15) of Ref. 50. (1 hartree/bohr^2=1.557×10^6 erg/cm^2).

r_s	2	3	4	6
σ_x^{LSDA}	3036	669	222	43.6
σ_x^{PBE}	2436	465	128	11.8
$\sigma_x^{\mathrm{PBEsol}}$	2666	540	162	22.9
σ_x^{TPSS}	2553	498	141	15.4
σ_x^{LAG}	2908	619	198	34.3
σ_x^{LAA}	2896	615	196	33.6
σ_x^{AM05}	2934	627	201	35.4
$\sigma_x^{\mathrm{ARPA+}}$	2941	626	199	34.6
σ_x^{exact}	2624	526	157	22
$\sigma_{\mathrm{xc}}^{\mathrm{LSD\text{-}RPA}}$	3403	781	269	56
$\sigma_{\mathrm{xc}}^{\mathrm{PBE\text{-}RPA}}$	3318	760	262	55
$\sigma_{\mathrm{xc}}^{\mathrm{ARPA}}$	3366	764	260	53
$\sigma_{\mathrm{xc}}^{\mathrm{RPA}}$	3467	801	278	58
$\sigma_{\mathrm{xc}}^{\mathrm{LSDA}}$	3354	764	261	53
$\sigma_{\mathrm{xc}}^{\mathrm{PBE}}$	3265	741	252	52
$\sigma_{\mathrm{xc}}^{\mathrm{PBEsol}}$	3374	774	267	56
$\sigma_{\mathrm{xc}}^{\mathrm{TPSS}}$	3380	772	266	55
$\sigma_{\mathrm{xc}}^{\mathrm{LAG}}$	3226	714	237	43.7
$\sigma_{\mathrm{xc}}^{\mathrm{AM05}}$	3414	782	270	56.7
$\sigma_{\mathrm{xc}}^{\mathrm{ARPA+}}$	3313	745	250	50
$\sigma_{\mathrm{xc}}^{\mathrm{RPA+}}$	3413	781	268	54
$\sigma_{\mathrm{xc}}^{\mathrm{DMC}}$	3392±50	768±10	261±8	52.5±…

In Fig. 10 we show $\epsilon_{\mathrm{xc}}^{\mathrm{RPA}}$ given by Eq. (12), $\epsilon_{\mathrm{xc}}^{\mathrm{ARPA}}$ given by Eq. (22), and $\epsilon_{\mathrm{xc}}^{\mathrm{PBE\text{-}RPA}}$ of Ref. 18 for two thick jellium slabs of bulk parameters r_s=2.07 and r_s=4. We use accurate LSDA orbitals and densities as in Refs. 26, 45, and 46. ARPA fits well the exact RPA until $s\approx 20$, showing that the Airy gas and the jellium surfaces are very close related, as expected.

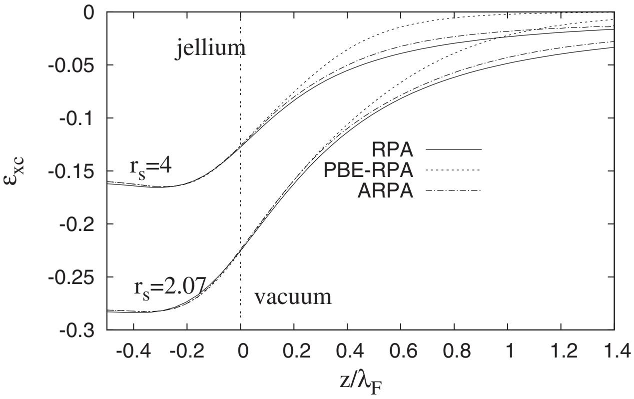

FIG. 10. RPA exchange-correlation energy (hartree) per particle ϵ_{xc} at position z versus z/λ_F at surfaces of two jellium slabs. The bulk parameters are r_s=2.07 and r_s=4. Both jellium slabs have the width $d=3.2\lambda_F$. The edges of the positive background are at $z=0$. The differences at large z, emphasized here by plotting ϵ_{xc} instead of $n\epsilon_{\mathrm{xc}}$, are not important for the surface energy.

In Table I we report the ARPA and ARPA+ jellium surface exchange and xc energies. The $\sigma_x^{\mathrm{ARPA+}}$ are close to but worse than σ_x^{LAG}. The $\sigma_{\mathrm{xc}}^{\mathrm{ARPA}}$ are between $\sigma_{\mathrm{xc}}^{\mathrm{RPA}}$ and $\sigma_{\mathrm{xc}}^{\mathrm{PBE\text{-}RPA}}$ for $r_s < \sim 3$ but lower than both others for $r_s > \sim 4$. The $\sigma_{\mathrm{xc}}^{\mathrm{ARPA+}}$ are reasonably close to $\sigma_{\mathrm{xc}}^{\mathrm{LSDA}}$ and $\sigma_{\mathrm{xc}}^{\mathrm{DMC}}$ (see Ref. 48) but are surprisingly lower and less accurate than $\sigma_{\mathrm{xc}}^{\mathrm{LSDA}}$.

B. Spherical atoms

In Table II we calculate the ARPA+ exchange and correlation energies of several atoms and ions. We use spin-restricted analytic Hartree-Fock orbitals[51] and densities. (The difference between Hartree-Fock orbitals and Kohn-Sham

TABLE II. Exchange and correlation energies (in hartrees) of several spherical atoms and ions with spin-restricted Hartree-Fock orbitals and densities (Ref. 51). Exact correlation energies are from Ref. 52. PBE GGA, not shown in the table, has the mean absolute errors (MAEs): 0.0476 for exchange and 0.01563 for correlation. (See also Table 5 of Ref. 44.)

	E_x^{LSDA}	$E_x^{\mathrm{ARPA+}}$	E_x^{HF}	E_c^{LSDA}	$E_c^{\mathrm{ARPA+}}$	E_c^{exact}
H	−0.268	−0.280	−0.313	−0.0222	−0.0199	0
He	−0.884	−0.925	−1.026	−0.1125	−0.1030	−0.0420
Li^+	−1.421	−1.486	−1.652	−0.1346	−0.1233	−0.0435
Be^{2+}	−1.957	−2.047	−2.277	−0.1504	−0.1378	−0.0443
Li	−1.538	−1.603	−1.781	−0.1508	−0.1378	−0.0453
Be^+	−2.168	−2.261	−2.507	−0.1727	−0.1578	−0.0474
Be	−2.312	−2.408	−2.667	−0.2240	−0.2058	−0.0943
B^+	−3.036	−3.157	−3.492	−0.2520	−0.2317	−0.1113
Ne^{6+}	−6.634	−6.886	−7.594	−0.3336	−0.3069	−0.1799
N	−5.893	−6.047	−6.596	−0.4273	−0.4016	−0.1883
Ne	−11.033	−11.220	−12.109	−0.7428	−0.7084	−0.3905
Ar	−27.863	−28.118	−30.190	−1.4242	−1.3723	−0.7222
MAE	0.600	0.481		0.1865	0.1664	

orbitals is small for atoms.) For every atom and ion of Table II, ARPA+GGA improves the LSDA results but it is still a poor approximation in comparison with GGA's constructed for atoms and molecules, such as PBE GGA.[3,15]

In Table III we show the xc contribution to the valence-shell removal energy (a quantity that can be accurately measured experimentally[44]) of three atoms (Li, Be, and Ne). We observe that the ARPA+ systematically improves the LSDA results, competing in accuracy with the PBE GGA.

C. Atomization energies of molecules

The AE6 test set[53] of atomization energies of molecules has only six molecules ($\mathrm{SiH_4}$, SiO, $\mathrm{S_2}$, $\mathrm{C_3H_4}$, $\mathrm{C_2H_2O_2}$, and $\mathrm{C_4H_8}$) and was constructed to reproduce the errors of density functionals for larger molecular sets, providing a quick but representative evaluation of the accuracy of density functionals for molecules. In Table IV we show the errors (in kcal/mol) of the AE6 atomization energies for ARPA+GGA, ARPA GGA, PBE GGA, PBEsol GGA, and AM05 GGA. The errors given by ARPA+GGA and ARPA GGA are practically the same, in accord with the work of Ref. 18, and show that the RPA+ short-range correction does not have an important effect on the atomization energies of molecules. Although our GGA short-range correction to RPA is important for total energies, it tends to cancel out of energy differences for processes in which the electron number remains unchanged (as in Tables I and IV but not Tables II and III). The accuracy of the ARPA+ for the AE6 test is close to that of PBEsol with both reducing the LSDA error by more than a factor of 2.

TABLE III. Change in xc energy (hartree) of an atom due to removal of a shell of valence electrons ($\Delta E_{\mathrm{xc}}=E_{\mathrm{xc}}^{atom}-E_{\mathrm{xc}}^{ion}$). The calculation is based on the exchange and correlation energies listed in Table II of this work and in Table VI of Ref. 44.

	$\Delta E_{\mathrm{xc}}^{\mathrm{LSDA}}$	$\Delta E_{\mathrm{xc}}^{\mathrm{ARPA+}}$	$\Delta E_{\mathrm{xc}}^{\mathrm{PBE}}$	$\Delta E_{\mathrm{xc}}^{exact}$
$\mathrm{Li}\to\mathrm{Li}^+$	−0.133	−0.132	−0.138	−0.131
$\mathrm{Be}\to\mathrm{Be}^{+2}$	−0.429	−0.430	−0.438	−0.440
$\mathrm{Ne}\to\mathrm{Ne}^{+6}$	−4.808	−4.737	−4.793	−4.726

While our ARPA overbinds molecules (and this overbinding is only slightly reduced in ARPA+), the full RPA apparently underbinds molecules.[55] Thus, even at the RPA level, the Airy-gas xc energy density does not seem to transfer very accurately to molecules: much better atomization energies are predicted by standard functionals such as the PBE GGA[15] or the TPSS meta-GGA.[47] GGA overbinding of molecules typically goes together with GGA underestimation of the magnitude of the exchange-correlation energy of an atom, which we found for LSDA and ARPA+ but not so much for PBE in Table II.

D. Equilibrium lattice constants of solids

In Table V we test the ARPA+GGA for a simple metal (Na), a semiconductor (Si), a transition metal (Cu), and an ionic solid (NaCl). The ARPA+GGA lattice constants are longer than the PBEsol ones, but shorter than the PBE values, except for NaCl where ARPA+ is close to PBE. These trends are plausible from the enhancement factors plotted in Figs. 6 and 7, and the maximum *s* values reported in Ref. 24. These calculations also suggest that the correct second-order gradient expansion for exchange,[57] employed in the construction of the PBEsol GGA, is the most promising path toward an accurate and nonempirical GGA for solids.

The GAUSSIAN03 code that we use gives lattice constants that are on average a little too long.[24] The LSDA lattice constants calculated with the more accurate WIEN2K code

TABLE IV. The errors (kcal/mole) of the atomization energies of the AE6 set of molecules. We use the $6-311+G(3df,2p)$ basis set in the GAUSSIAN03 code. The AM05 atomization energies of the AE6 set of molecules were calculated in Ref. 54, using the spin-polarized version of AM05 given in Ref. 17. The LSDA mean error (ME) is 77.3 kcal/mole and its MAE is 77.3 kcal/mole (Ref. 16). The TPSS meta-GGA of Ref. 47 gives ME=4.2 kcal/mole, and MAE=6.0 kcal/mole. The AE6 mean atomization energy is 517 kcal/mole. (1 hartree=627.5 kcal/mole.) (For ARPA+ and ARPA, we used PBEsol densities.)

	PBE	ARPA+	ARPA	PBEsol	AM05
SiH_4	−9.2	10.1	9.9	1.3	7.6
SiO	3.6	11.2	12.3	12.9	13.5
S_2	13.1	18.4	19.2	21.9	21.6
C_3H_4	16.4	46.0	50.6	45.1	48.1
$C_2H_2O_2$	31.8	60.1	65.7	64.7	66.6
C_4H_8	18.7	70.6	78.7	69.6	75.0
ME	12.4	36.1	39.4	35.9	38.7
MAE	15.5	36.1	39.4	35.9	38.7

are:[58] Na 4.047, Si 5.407, Cu 3.522, and NaCl 5.465. Thus, extensive and more accurate lattice constants calculations need to be performed for our ARPA+.

V. CONCLUSIONS

In this paper we construct the RPA correlation energy density of the Airy gas, using an accurate Airy-gas model that has only 19 occupied orbitals. This approach can be generalized to other physical systems, such as a more sophisticated edge electron gas that can include curvature corrections [arising from nonlinearity of $v_{eff}(z)$].

We have constructed the ARPA GGA that accurately fits the RPA xc energy density of the Airy gas and we have corrected its short-range part in the framework of the RPA + [18] approach, developing the ARPA+GGA entirely without empiricism. Because of the delocalization of the electrons in the Airy gas, our ARPA+GGA has nearly the correct Airy-gas correlation energy. Via Figs. 8 and 9, our ARPA+ confirms the AM05 hypothesis[14] for the correlation functional compatible with Airy-gas GGA exchange.[13,14]

By testing the ARPA+GGA for jellium surfaces, atoms, molecules, and bulk solids, we observe that the xc energy density of the Airy gas can be transferred successfully to a very similar system such as the jellium surface but less successfully to a very different system such as a bulk solid, an atom, or a molecule. However, the ARPA+GGA mildly improves the LSDA results for lattice constants and atomization energies, without much worsening the already good surface exchange-correlation energies.

We would have liked to replace the RPA+ method by the more sophisticated inhomogeneous Singwi-Tosi-Land-Sjőlander (ISTLS) (Refs. 49 and 59) but were not able to achieve sufficiently accurate numerical results for the correlation energy densities thereof. The future use of ISTLS could refine our input and provide an energy density (not just an integrated energy) for the short-range correction to RPA. Other possible future refinements could include the use of different reference systems for the bulk and surface of a solid,[14,19] replacing the Airy gas by a more sophisticated example of the edge electron gas, or replacing the GGA functional form by the meta-GGA.[47] We suspect[21,54] that the meta-GGA form is needed to achieve simultaneous high accuracy for atoms, molecules, and solids near equilibrium. In fact the TPSS meta-GGA[47,62] is already close to being such a general-purpose semilocal functional and a revised TPSS (Ref. 54) with improved lattice constants may be even closer.

TABLE V. Lattice constants (in Å) calculated with the GAUSSIAN03 code as in Ref. 16 and compared to experimental values corrected to the static-lattice limit (Refs. 16 and 56). (For ARPA+, we used PBEsol densities.)

Solid	LSDA	PBE	PBEsol	ARPA+	Exper.
Na	4.049	4.199	4.159	4.207	4.210
Si	5.410	5.479	5.442	5.470	5.423
Cu	3.530	3.635	3.578	3.605	3.596
NaCl	5.471	5.696	5.611	5.716	5.580
ME	−0.087	0.050	−0.005	0.045	
MAE	0.087	0.056	0.030	0.049	

We note however that there are two formally unsatisfactory aspects of using the exchange-correlation energy density of a nonuniform system as a reference for the construction of density functionals: (1) except in the uniform electron gas, the energy density is neither observable nor unique since any function integrating to zero can be added to it with no physical consequence. Here, as in Refs. 13, 14, 41, 60, and 61, we have chosen the conventional[62] gauge for the energy density but other choices should be explored. (2) While the integrated exchange energy for a slowly varying density is expressible in terms of the GGA ingredients n and ∇n, the conventional exchange energy density in this limit is not so expressible, having a Laplacian term $\nabla^2 n^{2/3}$ which integrates to zero but has a divergent coefficient.[19,63] As a result, the Airy-gas GGA cannot predict accurate exchange energies for slowly varying electron densities (e.g., the jellium surface exchange energy) while more standardly constructed GGAs-like PBEsol can do so[16] (our Table I). The Airy-gas GGA can at best work for the jellium surface by error cancellation between exchange and correlation, which is possible for typical valence-electron densities but not under uniform density scaling to the high-density limit where exchange dominates.

The GGA constructed here has no clear practical advantage over already published ones. Our purpose is not to advocate its use but to show what is obtained from the Airy-gas reference system within a consistent implementation for correlation as well as exchange.

ACKNOWLEDGMENTS

We thank Levente Vitos for providing us with the exact exchange energy per particle of the Airy gas, shown in Fig. 3 as the curve labeled “Airy gas.” We thank Ann Mattsson for comments on the manuscript. L.A.C. thanks J. M. Pitarke for many valuable discussions and suggestions. L.A.C. and J.P.P. acknowledge NSF support (Grant No. DMR05-01588).

---

[1] W. Kohn and L. J. Sham, Phys. Rev. **140**, A1133 (1965).
[2] W. Kohn and A. E. Mattsson, Phys. Rev. Lett. **81**, 3487 (1998).
[3] J. P. Perdew, L. A. Constantin, E. Sagvolden, and K. Burke, Phys. Rev. Lett. **97**, 223002 (2006).
[4] V. Sahni, C. Q. Ma, and J. S. Flamholz, Phys. Rev. B **18**, 3931 (1978).
[5] A. Solomatin and V. Sahni, Phys. Rev. B **56**, 3655 (1997).
[6] V. Sahni and K.-P. Bohnen, Phys. Rev. B **29**, 1045 (1984); **31**, 7651 (1985).
[7] R. Baltin, Z. Naturforsch. A **27A**, 1176 (1972).
[8] D. A. Kirzhnitz, Sov. Phys. JETP **5**, 64 (1957); D. A. Kirzhnitz, *Field Theoretical Methods in Many-Body Systems* (Pergamon, Oxford, 1967).
[9] M. Brack, B. K. Jennings, and Y. H. Chu, Phys. Lett. **65B**, 1 (1976).
[10] S. K. Ghosh and L. C. Balbas, J. Chem. Phys. **83**, 5778 (1985).
[11] L. Vitos, B. Johansson, J. Kollár, and H. L. Skriver, Phys. Rev. A **61**, 052511 (2000).
[12] L. A. Constantin and A. Ruzsinszky, Phys. Rev. B **79**, 115117 (2009).
[13] L. Vitos, B. Johansson, J. Kollár, and H. L. Skriver, Phys. Rev. B **62**, 10046 (2000).
[14] R. Armiento and A. E. Mattsson, Phys. Rev. B **72**, 085108 (2005).
[15] J. P. Perdew, K. Burke, and M. Ernzerhof, Phys. Rev. Lett. **77**, 3865 (1996).
[16] J. P. Perdew, A. Ruzsinszky, G. I. Csonka, O. A. Vydrov, G. E. Scuseria, L. A. Constantin, X. Zhou, and K. Burke, Phys. Rev. Lett. **100**, 136406 (2008).
[17] A. E. Mattsson and R. Armiento, Phys. Rev. B **79**, 155101 (2009).
[18] Z. Yan, J. P. Perdew, and S. Kurth, Phys. Rev. B **61**, 16430 (2000).
[19] R. Armiento and A. E. Mattsson, Phys. Rev. B **66**, 165117 (2002).
[20] A. E. Mattsson, R. Armiento, and T. R. Mattsson, Phys. Rev. Lett. **101**, 239701 (2008).
[21] J. P. Perdew, A. Ruzsinszky, G. I. Csonka, O. A. Vydrov, G. E. Scuseria, L. A. Constantin, X. Zhou, and K. Burke, Phys. Rev. Lett. **101**, 239702 (2008).
[22] A. E. Mattsson, R. Armiento, J. Paier, G. Kresse, J. M. Wills, and T. R. Mattsson, J. Chem. Phys. **128**, 084714 (2008).
[23] M. Ropo, K. Kokko, and L. Vitos, Phys. Rev. B **77**, 195445 (2008).
[24] G. I. Csonka, J. P. Perdew, A. Ruzsinszky, P. H. T. Philipsen, S. Lebegue, J. Paier, O. A. Vydrov, and J. G. Angyan, Phys. Rev. B **79**, 155107 (2009).
[25] A linear effective potential does not imply a linear external potential. A quantum Monte Carlo calculation of the correlation energy density would have to start from the external potential.
[26] J. M. Pitarke and A. G. Eguiluz, Phys. Rev. B **57**, 6329 (1998); **63**, 045116 (2001).
[27] D. C. Langreth and J. P. Perdew, Phys. Rev. B **15**, 2884 (1977); **21**, 5469 (1980); **26**, 2810 (1982).
[28] O. Gunnarsson and B. I. Lundqvist, Phys. Rev. B **13**, 4274 (1976).
[29] J. Harris and A. Griffin, Phys. Rev. B **11**, 3669 (1975).
[30] E. K. U. Gross, J. F. Dobson, and M. Petersilka, in *Density Functional Theory II*, Topics in Current Chemistry Vol. 181, edited by R. F. Nalewajski (Springer, Berlin, 1996), p. 81.
[31] L. A. Constantin and J. M. Pitarke, Phys. Rev. B **75**, 245127 (2007).
[32] J. M. Pitarke and J. P. Perdew, Phys. Rev. B **67**, 045101 (2003).
[33] J. Jung, P. García-González, J. F. Dobson, and R. W. Godby, Phys. Rev. B **70**, 205107 (2004).
[34] L. A. Constantin and J. M. Pitarke, J. Chem. Theory Comput. **5**, 895 (2009).
[35] J. F. Dobson, H. M. Le, and G. Vignale, Phys. Rev. B **70**, 205126 (2004).
[36] A. G. Eguiluz, Phys. Rev. B **31**, 3303 (1985).
[37] We use a grid of 350 points nonuniformly distributed on the z axis. Our grid gives accurate RPA correlation energy densities for the region of interest $s \geq 0.3$. Calculations with 70 and 90 unoccupied orbitals and with 450 grid points give unchanged

RPA correlation energy densities for $s \geq 0.3$. The biggest error of our numerical calculation is in the region $s \leq 0.3$, where the Thomas-Fermi approximation becomes accurate.

[38] G. L. Oliver and J. P. Perdew, Phys. Rev. A **20**, 397 (1979).

[39] W. H. Press, S. A. Teukolsky, W. T. Vetterling, and B. P. Flannery, *Numerical Recipes* (Cambridge Univeristy Press, Cambridge, 1986).

[40] J. P. Perdew and Y. Wang, Phys. Rev. B **45**, 13244 (1992).

[41] J. P. Perdew, L. A. Constantin, and A. Ruzsinszky, Prog. Theor. Chem. Phys. (to be published).

[42] The numerical RPA conventional correlation energy density depends significantly on the slope value F when plotted against the standard reduced gradient for the correlation energy $t = |\nabla n| / [4(3/\pi)^{1/6} n^{7/6}]$. Thus the Airy-gas correlation energy density is better described by s_c of Eq. (20) or even by s of Eq. (11) (as proposed in AM05 GGA) than the standard reduced gradient for correlation t that was derived in the linear response of the uniform electron gas.

[43] J. P. Perdew, M. Ernzerhof, A. Zupan, and K. Burke, J. Chem. Phys. **108**, 1522 (1998).

[44] J. P. Perdew, J. Tao, V. N. Staroverov, and G. E. Scuseria, J. Chem. Phys. **120**, 6898 (2004).

[45] L. A. Constantin, J. P. Perdew, and J. M. Pitarke, Phys. Rev. B **79**, 075126 (2009).

[46] J. M. Pitarke, L. A. Constantin, and J. P. Perdew, Phys. Rev. B **74**, 045121 (2006).

[47] J. Tao, J. P. Perdew, V. N. Staroverov, and G. E. Scuseria, Phys. Rev. Lett. **91**, 146401 (2003).

[48] B. Wood, N. D. M. Hine, W. M. C. Foulkes, and P. García-González, Phys. Rev. B **76**, 035403 (2007).

[49] L. A. Constantin, J. M. Pitarke, J. F. Dobson, A. García-Lekue, and J. P. Perdew, Phys. Rev. Lett. **100**, 036401 (2008).

[50] L. M. Almeida, J. P. Perdew, and C. Fiolhais, Phys. Rev. B **66**, 075115 (2002).

[51] E. Clementi and C. Roetti, At. Data Nucl. Data Tables **14**, 177 (1974).

[52] S. J. Chakravorty, S. R. Gwaltney, E. R. Davidson, F. A. Parpia, and C. F. Fischer, Phys. Rev. A **47**, 3649 (1993); E. R. Davidson, S. A. Hagstrom, S. J. Chakravorty, V. M. Umar, and C. F. Fischer, *ibid.* **44**, 7071 (1991).

[53] B. J. Lynch and D. G. Truhlar, J. Phys. Chem. A **107**, 8996 (2003); **108**, 1460(E) (2004).

[54] J. P. Perdew, A. Ruzsinszky, G. I. Csonka, L. A. Constantin, and J. Sun, Phys. Rev. Lett. **103**, 026403 (2009).

[55] F. Furche, Phys. Rev. B **64**, 195120 (2001).

[56] A. B. Alchagirov, J. P. Perdew, J. C. Boettger, R. C. Albers, and C. Fiolhais, Phys. Rev. B **63**, 224115 (2001).

[57] P. R. Antoniewicz and L. Kleinman, Phys. Rev. B **31**, 6779 (1985).

[58] P. Haas, F. Tran, and P. Blaha, Phys. Rev. B **79**, 085104 (2009); P. Haas, F. Tran, and P. Blaha, *ibid.* **79**, 209902 (2009)

[59] J. F. Dobson, J. Wang, and T. Gould, Phys. Rev. B **66**, 081108(R) (2002).

[60] A. C. Cancio and M. Y. Chou, Phys. Rev. B **74**, 081202(R) (2006).

[61] R. Q. Hood, M. Y. Chou, A. J. Williamson, G. Rajagopal, R. J. Needs, and W. M. C. Foulkes, Phys. Rev. Lett. **78**, 3350 (1997).

[62] J. Tao, V. N. Staroverov, G. E. Scuseria, and J. P. Perdew, Phys. Rev. A **77**, 012509 (2008).

[63] J. P. Perdew and Y. Wang, in *Mathematics Applied to Science*, edited by J. A. Goldstein, S. Rosencrans, and G. Sod (Academic, New York, 1988).